

Utilization of Protruded Strip Resonators to Design a Compact UWB Antenna with WiMAX and WLAN Notch Bands

J. Mazloun¹ and N. Ojaroudi²

¹Electrical Engineering Department
Shahid Sattari Aeronautical University of Science and Technology, Tehran, Iran

²Young Researchers and Elite Club, Ardabil Branch
Islamic Azad University, Ardabil, Iran
n.ojaroudi@yahoo.com

Abstract — In this paper, a new design of ultra-wideband (UWB) microstrip monopole antenna is presented. The main novelty of the proposed structure is the using of protruded strips as resonators to design an UWB antenna with dual band-stop property. In the proposed design, by cutting the rectangular slot with a pair of rotated Y-shaped strips in the ground plane, additional resonance is excited and much wider impedance bandwidth can be achieved. To make a single band-notched function, the square radiating patch is converted to the square-ring structure with a pair of protruded fork-shaped strips. Finally, by cutting a rectangular slot with a protruded M-shaped strip at the feed line, a desired dual band-notched function is achieved. The measured results reveal that the presented dual band-notched antenna offers a very wide bandwidth from 2.8 to 11.6 GHz, with two notched bands, around of 3.3-3.7 GHz and 5-6 GHz covering all WiMAX and WLAN bands.

Index Terms — Dual band-notched antenna, protruded strip resonators, UWB system.

I. INTRODUCTION

UWB communication systems usually require smaller antenna size in order to meet the miniaturization requirements of the radio-frequency (RF) units [1]. It is rapidly advancing as a high data rate wireless communication technology. The Federal Communication Commission (FCC) has released a bandwidth of 7.5 GHz (from 3.1 GHz to 10.6 GHz) for ultra wideband wireless communications. Due to its high bandwidth and very short pulses, UWB radio wave propagation provides very high data rate which may be up to several hundred Megabits per seconds (Mbps), and it is difficult to tract the transmitting data, which highly ensures the data security. The UWB technology has another advantage from the power consumption point of view. Due to spreading the energy of the UWB signals over a large

frequency band, the maximum power available to the antenna as part of UWB system will be as small as in order of 0.5 mW according to the FCC spectral mask. This power is considered to be a small value and it is actually very close to the noise floor compared to what is currently used in different radio communication systems. It is a well-known fact that planar antennas present really appealing physical features, such as simple structure, small size, and low cost. Due to all these interesting characteristics, planar antennas are extremely attractive to be used in emerging UWB applications, and growing research activity is being focused on them. Consequently, a number of planar microstrip antennas have been experimentally characterized [2-4].

The frequency range for UWB systems between 3.1–10.6 GHz [5] will cause interference to the existing wireless communication systems, for example the wireless local area network (WLAN) for IEEE 802.11a operating in 5.15–5.35 GHz and 5.725–5.825 GHz bands, the worldwide interoperability microwave access (WiMAX) operating in 3.3–3.7 GHz and 5.35-5.65 GHz, so the UWB antenna with a band-notched function is required. Lately to generate the frequency band-notched function, several band-notched microstrip antennas have been reported [6-11].

All of the above methods are used for rejecting a single band of frequencies. However, to effectively utilize the UWB spectrum and to improve the performance of the UWB system, it is desirable to design the antenna with dual band rejection. It will help to minimize the interference between the narrow band systems with the UWB system. Some methods are used to obtain the dual band rejection in the literature [12-15].

In this paper, a new monopole antenna with dual band-notched characteristic for UWB applications has been proposed. The proposed antenna consists of a square-ring radiating stub with a pair of protruded fork-shaped strips, a feed-line with an M-shaped strip

protruded inside the rectangular slot, and a ground plane with a pair of protruded Y-shaped strips inside the slot.

II. ANTENNA DESIGN

The presented small monopole antenna fed by a microstrip line as shown in Fig. 1, is printed on an FR4 substrate of thickness 1.6 mm, permittivity 4.4, and loss tangent 0.018.

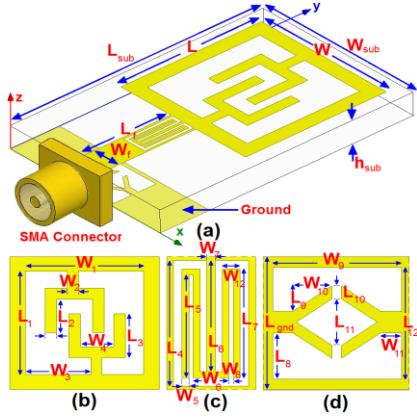


Fig. 1. Geometry of the proposed monopole antenna: (a) side view, (b) radiating patch, (c) feed-line, and (d) modified DGS.

The basic monopole antenna structure consists of a square patch, a feed line, and a ground plane. The square patch has a width W . The patch is connected to a feed line of width W_f and length L_f . On the other side of the substrate, a conducting ground plane is placed.

Regarding defected ground structures (DGS) theory, the creating slots in the ground plane provide additional current paths. Moreover, these structures change the inductance and capacitance of the input impedance, which in turn leads to change the bandwidth [16]. Therefore, by cutting a rectangular slot with a pair of rotated Y-shaped strips in the ground plane, much enhanced impedance bandwidth may be achieved. In the proposed design, protruded Y-shaped strips in the ground plane are used to make an additional resonance and increase the bandwidth.

This work started by choosing the dimensions of the designed antenna. Hence, the essential parameters for the design are: $f_0 = 4.5$ GHz (first resonance frequency), $\epsilon_r = 4.4$ and $h_{sub} = 0.8$ mm. The dimensions of the patch along its length have now been extended on each end by a distance ΔL , which is given as:

$$\Delta L = 0.412 h_{sub} \frac{(\epsilon_{eff} + 0.3) \left(\frac{W_{sub}}{h_{sub}} + 0.264 \right)}{(\epsilon_{eff} - 0.258) \left(\frac{W_{sub}}{h_{sub}} + 0.8 \right)}, \quad (1)$$

where h_{sub} is the height of dielectric, W_{sub} is the width of the microstrip monopole antenna and $\epsilon_{r_{eff}}$ is the effective dielectric constant. Then, the effective length (L_{eff}) of the patch can be calculated as follows:

$$L_{eff} = L + 2\Delta L. \quad (2)$$

For a given resonant frequency f_0 , the effective length is given as:

$$L_{eff} = \frac{C}{2f_0 \sqrt{\epsilon_{r_{eff}}}}. \quad (3)$$

For a microstrip antenna, the resonance frequency for any TM_{mn} mode is given by as:

$$\epsilon_{eff} = \frac{(\epsilon_r + 1) + (\epsilon_r - 1) \left[1 + 12 \frac{h_{sub}}{W_{sub}} \right]^{-1}}{2}. \quad (4)$$

The width W_{sub} of microstrip antenna is given:

$$W_{sub} = \frac{C}{2f_0 \sqrt{(\epsilon_r + 1)}}. \quad (5)$$

The last and final step in the design is to choose the length of the resonator and the band-stop filter elements. In this design, the optimized length $L_{resonance}$ is set to resonate at $0.25\lambda_{resonance}$, where $L_{resonance} = L_9 + L_{12} - L_8 + W_{11} + 0.5W_{10}$. $\lambda_{resonance}$ corresponds to the extra resonance frequency (12 GHz), respectively. Also, the optimized length L_{notch} is set to band-stop resonate at $0.5\lambda_{notch}$, where $L_{notch1} = L_5 + W_5 + W_{12} + 0.5(L_4 + L_6 + W_6)$, and $L_{notch2} = 0.5(L_1 + W_1) + L_2 + W_2 + W_4$. λ_{notch1} and λ_{notch2} correspond to first band-notched frequency (3.5 GHz) and second band-notched frequency (5.5 GHz), respectively. The final values of proposed design parameters are specified in Table 1.

Table 1: Final dimensions of antenna parameters

Parameter	W	L	W_1	L_1
Value (mm)	10	10	8	8
Parameter	W_2	L_2	W_3	L_3
Value (mm)	0.5	3.1	4.5	3.6
Parameter	W_4	L_4	W_5	L_5
Value (mm)	2	3.5	0.2	3
Parameter	W_6	L_6	W_7	L_7
Value (mm)	1	3.1	0.2	3.1
Parameter	W_8	L_8	W_9	L_9
Value (mm)	0.15	1.25	4	0.75
Parameter	W_{10}	L_{10}	W_{11}	L_{11}
Value (mm)	1.25	0.3	0.75	2.8
Parameter	W_{12}	L_{12}	W_f	L_f
Value (mm)	0.55	3	7	2
Parameter	W_{sub}	L_{sub}	h_{sub}	L_{gnd}
Value (mm)	12	18	1.6	3.5

In the square-ring stub, two fork-shaped strips protruded inside the ring have been used for generating

a single band-stop performance that's playing an important role in the broadband characteristics of this antenna, because by using it, the band-notch performance can be controlled such as band-rejections range and variable function. The modified M-shaped strip protruded inside rectangular slot at feed-line causes a second band-notched performance which finally a multi-resonance antenna with desired dual band-notched function to suppress interferences from WLAN, WiMAX, and C-bands can be achieved [11].

III. RESULTS AND DISCUSSIONS

The planar monopole antenna with various design parameters was constructed, and the numerical and experimental results of the input impedance and radiation characteristics are presented and discussed. The analysis and performance of the proposed antenna is examined by using Ansoft simulation software high-frequency structure simulator (HFSS) [17], for better impedance matching.

VSWR characteristics for the ordinary monopole antenna [Fig. 2 (a)], the antenna with a pair of rotated Y-shaped strips protruded inside the slot at ground plane [Fig. 2 (b)], the square-ring antenna with pairs of protruded Y-shaped and fork-shaped strips [Fig. 2 (c)], and the proposed antenna structure [(Fig. 2 (d)] are compared in Fig. 3.

As shown in Fig. 3, by using the pair of rotated Y-shaped strips at the ground plane, a new resonance at the higher frequency (10.7 GHz) is generated and the usable upper frequency of the antenna is extended from 10.3 GHz to 11.9 GHz. To generate a single frequency band-notched function, the square radiating patch was converted to the square-ring structure with a pair of protruded fork-shaped strips, and also by using an M-shaped strip inside the rectangular slot at feed-line, the good dual band-notched function can be achieved which is covering the 3.5/5.5 GHz WiMAX/WLAN bands [11-13].

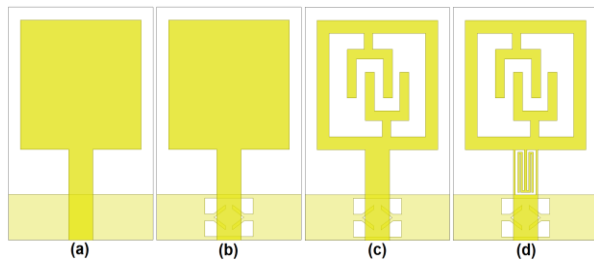


Fig. 2. (a) Ordinary monopole antenna, (b) antenna with pair of Y-shaped strips, (c) antenna with pairs of Y-shaped and fork-shaped strips, and (d) the proposed monopole antenna.

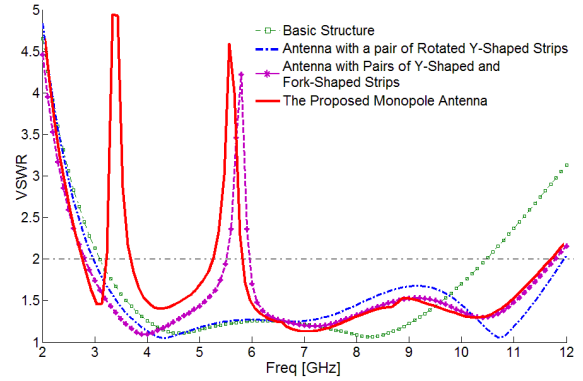


Fig. 3. Simulated VSWR characteristics for the various structures shown in Fig. 2.

To understand the phenomenon behind the multi resonance and dual band-notched performances, the simulated current distribution for the proposed antenna at the new resonance frequency (9.5 GHz) and notched frequencies (3.5 & 5.5 GHz) is presented in Fig. 4. It can be observed on Fig. 4 (a), at 10.5 GHz the current concentrated on the edges of the interior and exterior of the Y-shaped strips protruded inside the slot. Therefore, the antenna impedance changes at these frequencies due to the resonance properties of the proposed structure.

Figures 4 (a) and 4 (b) present the simulated current distributions on the top layer at the notched frequencies (3.7 and 5.5 GHz). As illustrated in Figs. 4 (b) and 4 (c), at the notched frequencies, the current flows are more dominant around of the fork-shaped and M-shaped strips. As a result, the desired high attenuation near the notched frequencies can be produced [18-19]. As seen in these figures, the current direction on the reject structures is opposite to each other, so the far fields produced by the currents on the reject structures cancel out each other in the reject band.

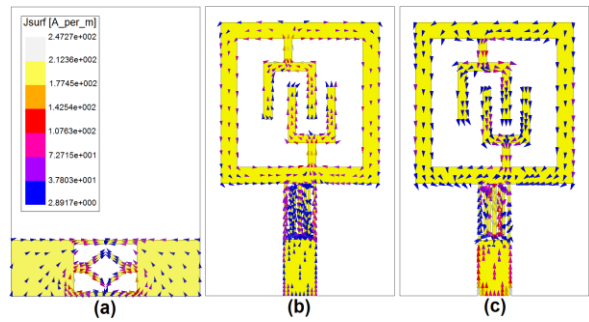


Fig. 4. Simulated surface current: (a) at 10.7 GHz (first extra resonance frequency), (b) at 3.5 GHz (first notched frequency), and (c) at 5.5 GHz (second notched frequency).

The proposed antenna with final design as shown in Fig. 5, was built and tested. The VSWR characteristic of the antenna was measured using the HP 8720ES network analyzer in an anechoic chamber. The radiation patterns have been measured inside an anechoic chamber using a double-ridged horn antenna as a reference antenna placed at a distance of 2 m. Also, two-antenna technique using an Agilent E4440A spectrum analyzer and a double-ridged horn antenna as a reference antenna placed at a distance of 2 m is used to measure the radiation gain in the z axis direction (x-z plane). Measurement set-up of the proposed antenna for the VSWR, antenna gain and radiation pattern characteristics are shown in Fig. 6.

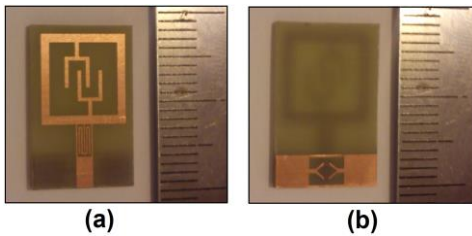


Fig. 5. Fabricated antenna: (a) top view, and (b) bottom view.

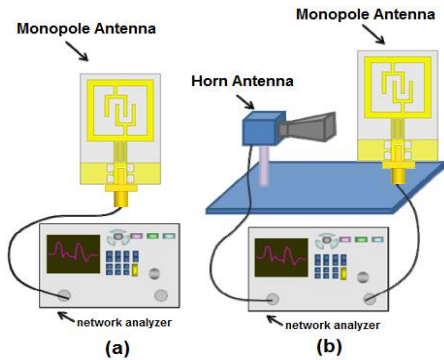


Fig. 6. Measurement set-up of the antenna: (a) VSWR, and (b) antenna gain and radiation patterns.

Figure 7 shows the measured and simulated VSWR characteristics of the proposed antenna. The antenna has the frequency band of 2.8 to 11.8 GHz with two rejection bands around 3.3.-3.7 and 5-6 GHz.

Figure 8 depicts the measured and simulated radiation patterns of the proposed antenna including the co-polarization and cross-polarization in the H-plane (x-z plane) and E-plane (y-z plane). It can be seen that quasi-omnidirectional radiation pattern can be observed on x-z plane over the whole UWB frequency range, especially at the low frequencies. The radiation patterns on the y-z plane display a typical figure-of-eight (8), similar to that of a conventional dipole antenna. The radiating patterns indicated at higher frequencies have

more ripples in both E- and H-planes, owing to generation of higher-order modes [20-21]. Measured and simulated maximum gains of the proposed antenna are shown in Fig. 9. Two sharp decrease of maximum gains in the notched frequencies bands at 3.5 and 5.5 GHz are shown in Fig. 9. For other frequencies outside the notched frequencies, the antenna gains has a flat property which increases by the frequency. As illustrated, the proposed antenna has sufficient and acceptable gain level in the operation bands [22].

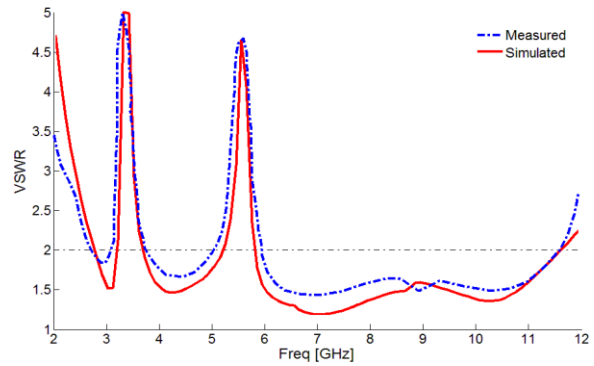


Fig. 7. Measured and simulated VSWR characteristics of the proposed antenna.

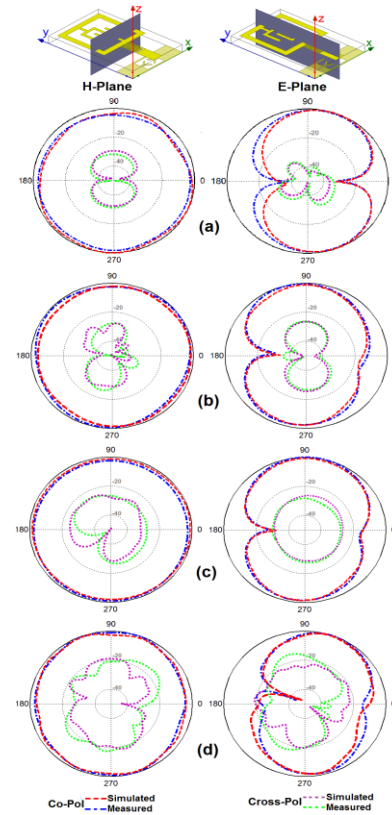


Fig. 8. Measured and simulated radiation patterns: (a) 3 GHz, (b) 4.5 GHz, (c) 7 GHz, and (d) 11 GHz.

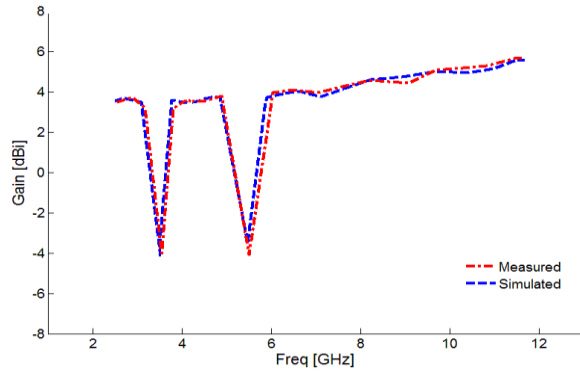


Fig. 9. Measured and simulated gains of the proposed antenna.

The measured and simulated radiation efficiency characteristic of the proposed antenna is shown in Fig. 10. The efficiency measurement was conducted using the reverberation chamber a cavity-technique and based approach, called the source-stirred method. Measured and also simulated results of the calculations using the software HFSS indicated that the proposed antenna features a good efficiency, being greater than 87% across the entire radiating band except in two notched bands [23]. On the other hand, the radiation efficiencies of the proposed dual band-notched antenna at 3.5 and 5.5 GHz, are only about 29 and 31%, respectively.

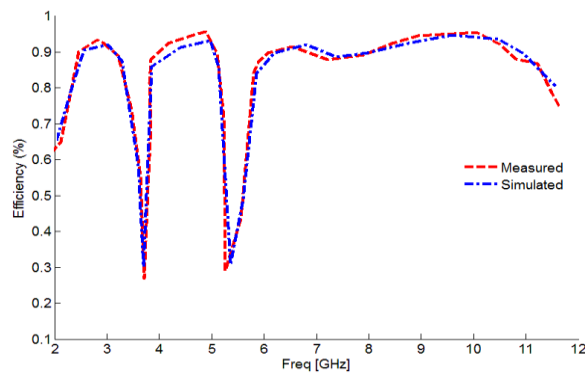


Fig. 10. Measured and simulated radiation efficiency characteristic of the proposed antenna.

IV. CONCLUSION

In this paper, a novel small monopole antenna with WiMAX/WLAN band-stop characteristic for UWB applications is proposed. In this design, the proposed antenna can operate from 2.8 to 11.8 GHz with two rejection bands around 3.3 to 3.7 GHz and 5 to 6 GHz. The designed antenna has a small size of $12 \times 18 \times 1.6 \text{ mm}^3$. Good VSWR and radiation pattern characteristics are obtained in the frequency band of interest.

REFERENCES

- [1] D. Cheng, *Compact Ultra Wideband Microstrip Resonating Antenna*, US Patent 7872606, Jan. 2011.
- [2] N. Ojaroudi, M. Ojaroudi, and N. Ghadimi, "UWB omnidirectional square monopole antenna for use in circular cylindrical microwave imaging systems," *IEEE Antennas Wireless Propag. Lett.*, vol. 11, pp. 1350-1353, 2012.
- [3] N. Ojaroudi, "Compact UWB monopole antenna with enhanced bandwidth using rotated L-shaped slots and parasitic structures," *Microw. Opt. Technol. Lett.*, vol. 56, pp. 175-178, 2014.
- [4] N. Ojaroudi, "Bandwidth improvement of monopole antenna using π -shaped slot and conductor-backed plane," *International Journal of Wireless Communications, Networking and Mobile Computing*, vol. 1, no. 2, pp. 14-19, 2014.
- [5] FCC News Release, FCC NEWS (FCC 02-48), Feb. 14, 2002.
- [6] N. Ojaroudi, "Application of protruded strip resonators to design an UWB slot antenna with WLAN band-notched characteristic," *Progress in Electromagnetics Research C*, vol. 47, pp. 111-117, 2014.
- [7] H. Mardani, C. Ghobadi, and J. Nourinia, "A simple compact monopole antenna with variable single-and double-filtering function for UWB applications," *IEEE Antennas and Wireless Propagation Letters*, vol. 9, pp. 1076-1079, 2010.
- [8] N. Ojaroudi, "A modified compact microstrip-fed slot antenna with desired WLAN band-notched characteristic," *American Journal of Computation, Communication and Control*, vol. 1, no. 3, pp. 56-60, 2014.
- [9] N. Ojaroudi and M. Ojaroudi, "An UWB slot antenna with band-stop notch," *IET Microw. Antennas Propag.*, vol. 10, pp. 831-835, 2013.
- [10] N. Ojaroudi, S. Amiri, and F. Geran, "A novel design of reconfigurable monopole antenna for UWB applications," *Applied Computational Electromagnetics Society (ACES) Journal*, vol. 28, no. 6, pp. 633-639, July 2013.
- [11] N. Ojaroudi, "Frequency reconfigurable microstrip antenna integrated with PIN diodes for cognitive radio," *22nd Telecommunications Forum, TELFOR 2014*, Belgrade, Serbia, Nov. 25-27, 2014.
- [12] N. Ojaroudi, "Microstrip monopole antenna with dual band-stop function for UWB applications," *Microw. Opt. Technol. Lett.*, vol. 56, pp. 818-822, 2014.
- [13] N. Ojaroudi, "Application of protruded Γ -shaped strips at the feed-line of UWB microstrip antenna to create dual notched bands," *International Journal of Wireless Communications, Networking*

- and Mobile Computing*, vol. 1, no. 1, pp. 8-13, 2014.
- [14] N. Ojaroudi, "An UWB microstrip antenna with dual band-stop performance using a meander-line resonator," *22nd International Conference on Software, Telecommunications and Computer Networks (SoftCOM)*, Croatia, 2014.
- [15] N. Ojaroudi, "Design of small reconfigurable microstrip antenna for UWB-CR applications," *19th International Symposium on Antenna and propagation, ISAP2014*, Kaohsiung, Taiwan, Dec. 2-5, 2014.
- [16] N. Ojaroudi, "Microstrip-fed antenna design for use in circular cylindrical microwave imaging applications," *22nd Telecommunications Forum, TELFOR 2014*, Belgrade, Serbia, Nov. 25-27, 2014.
- [17] Ansoft High Frequency Structure Simulator (HFSS), ver. 13, Ansoft Corporation, Pittsburgh, PA, 2010.
- [18] N. Ojaroudi, "Small microstrip-fed slot antenna with frequency band-stop function," *21st Telecommunications Forum, TELFOR 2013*, Belgrade, Serbia, Nov. 27-28, 2013.
- [19] N. Ojaroudi, "Novel design of low-profile microstrip band-stop filter (BSF) with Koch fractal RSLRs," *22nd Telecommunications Forum, TELFOR 2014*, Belgrade, Serbia, Nov. 25-27, 2014.
- [20] N. Ojaroudi, "New design of multi-band PIFA for wireless communication systems," *19th International Symposium on Antenna and propagation, ISAP 2014*, Kaohsiung, Taiwan, Dec. 2-5, 2014.
- [21] N. Ojaroudi, "Design of ultra-wideband monopole antenna with enhanced bandwidth," *21st Telecommunications Forum, TELFOR 2013*, Belgrade, Serbia, Nov. 27-28, 2013.
- [22] N. Ojaroudi, "Design of microstrip antenna for 2.4/5.8 GHz RFID applications," *German Microwave Conference, GeMic 2014*, Germany, 2014.
- [23] N. Ojaroudi and M. Ojaroudi, "Novel design of dual band-notched monopole antenna with bandwidth enhancement for UWB applications," *IEEE Antennas Wireless Propag. Lett.*, vol. 12, pp. 698-701, 2013.